iScience

CellPress
OPEN ACCESS

Article

Climate and cultural evolution drove Holocene cropland change in the Huai River Valley, China

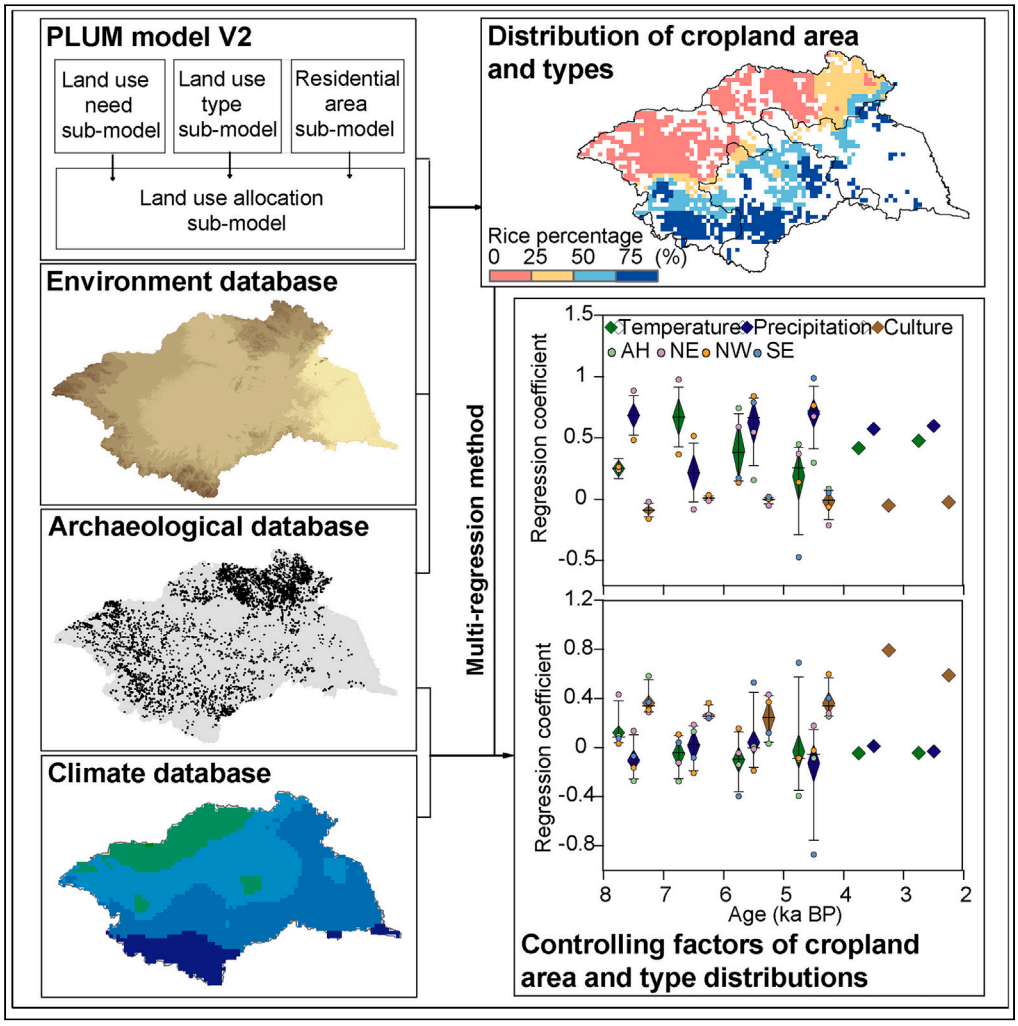

Yanyan Yu, Haibin Wu, Wenchao Zhang, ..., Chenglong Deng, Junyi Ge, Zhengtang Guo

yyy@mail.iggcas.ac.cn

Highlights

Improved PLUM2 reconstructs both cropland type and area

Cropland in the Huai River Valley expanded obviously during 5-4 and 3–2 ka BP

Boundary of rice-dominated cultivation shifted with climate change

Cultural intensity controlled the change of cropland area

Yu et al., iScience 27, 110841
October 18, 2024
https://doi.org/10.1016/j.isci.2024.110841

iScience

CellPress
OPEN ACCESS

Article

Climate and cultural evolution drove Holocene cropland change in the Huai River Valley, China

Yanyan Yu,[1,10,*] Haibin Wu,[1,2] Wenchao Zhang,[3] Nicole Boivin,[4,5,6] Jie Yu,[1] Juzhong Zhang,[7] Xin Zhou,[8] Wuhong Luo,[7] Chenglong Deng,[1] Junyi Ge,[9] and Zhengtang Guo[1]

SUMMARY

As an important way of maximizing land productivity by growing more than one crop type in the same field, mixed cropping has been an effective option for sustaining population growth under different climatic conditions since prehistoric period. We used a combination of archaeological data and an improved prehistoric land use model (PLUM) to quantitatively reconstruct spatiotemporal changes in cropland types and areas in the Huai River Valley of China, a core region of mixed cropping during the Holocene. The total cropland area increased more than 25 times during 8–2 ka BP, with northward expansion of rice-dominated cultivation during 5–4 ka BP and southward expansion of dry-dominated cultivation after 4 ka BP. Temperature and precipitation determined cropland types distribution, while that of cropland area was controlled by cultural development. The interplay between past climate, culture, and cultivation potentially provides useful insights into mitigating future population pressures with climate change.

INTRODUCTION

Croplands are the basis for much of the world's food production, supplying over 90% of global food calories.[1] Mixed cropping, including intercropping, is the oldest form of systemized agricultural production and involves the growing of two or more species, or cultivars of the same species, simultaneously in the same field.[2] It is practiced as an important means of maximizing land productivity through the intensification of cropping in the spatial domain.[3] Accordingly, mixed cropping has been widely utilized across China, India, Africa, and Latin America over a long period,[4,5] with important implications for regional population growth and cultural development.[6,7]

China is one of the three major regions of agricultural origins in the world (Figure 1A).[8] The expansion of millet cultivation from the Yellow River Valley, and rice cultivation from the Yangtze River Valley, led to the formation of the world's earliest mixed cropping system in central China by 8000 a BP.[9–13] This typical mixed cropping area is situated in the transitional zone between the humid and semi-humid climatic regimes in China,[12] and hence it is sensitive to climate change, while also acting as a key crossroad for regional trade and communication (Figure 1B; Table S1).[14] Thus, research aimed at better understanding the mechanisms of spatiotemporal cropland change in central China during the Holocene may also provide insights into the long-term co-evolution of human activity, climate, and culture in this region.

The roles of both climate change and cultural factors in driving cropland expansion have been examined in various archaeological studies.[15–23] The relative contributions of climatic and cultural factors to the evolution of the distribution of cropland, however, remain to be clarified, as most of current studies focus on comparisons of the curves of different variables over time.[15–21,23] While several archaeobotanical studies have provided semi-quantitative insights into changes in the spatial pattern of cropland types through time based on point records,[12,22,24,25] there are limited reliable quantitative data about changes in the distributions of cropland type and area, which hinders the assessment of the relative roles of climate, culture, and other factors in cropland evolution. For mixed cropping areas, it is particularly important to clarify changes in both cropland type and area, as these variables were potentially controlled by different factors.[12,22]

[1]State Key Laboratory of Lithospheric and Environmental Coevolution, Institute of Geology and Geophysics, Chinese Academy of Sciences, Beijing 100029, China
[2]University of Chinese Academy of Sciences, Beijing 100049, China
[3]School of Earth Sciences and Resources, China University of Geosciences (Beijing), Beijing 100083, China
[4]Department of Archaeology, Max Planck Institute for Geoanthropology, Jena 07745, Germany
[5]School of Social Science, University of Queensland, Brisbane, QLD 4072, Australia
[6]School of Environment and Science, Griffith University, Brisbane, QLD 4111, Australia
[7]School of Humanities and Social Sciences, University of Science and Technology of China, Hefei 230026, China
[8]School of Earth and Space Sciences, University of Science and Technology of China, Hefei 230026, China
[9]Key Laboratory of Vertebrate Evolution and Human Origins, Institute of Vertebrate Paleontology and Paleoanthropology, Chinese Academy of Sciences, Beijing 100044, China
[10]Lead contact
*Correspondence: yyy@mail.iggcas.ac.cn
https://doi.org/10.1016/j.isci.2024.110841

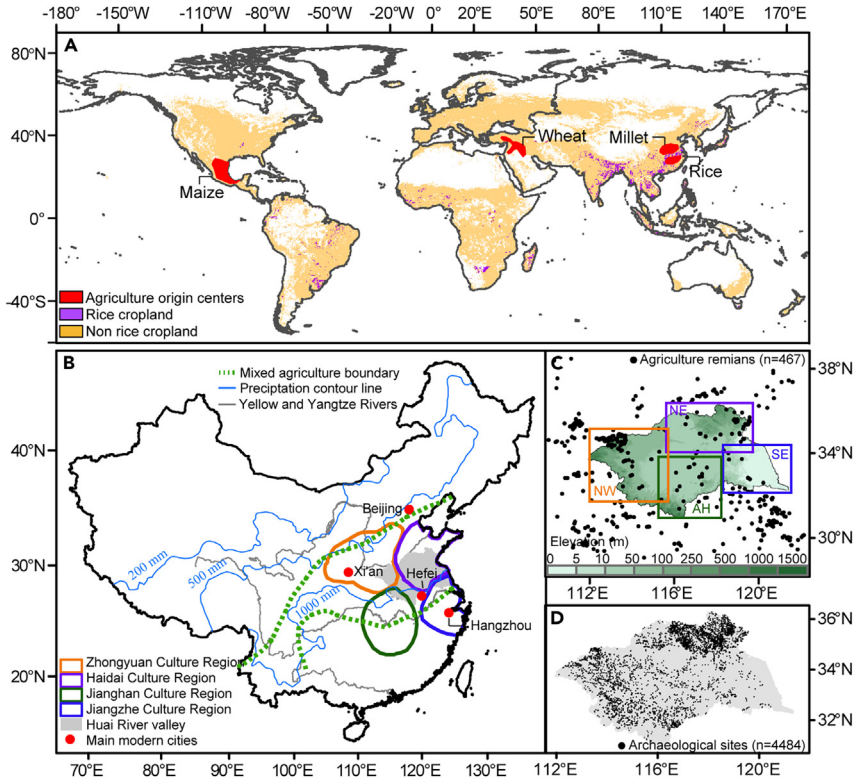

Figure 1. Spatial information for the study region

(A) Distribution of the centers of agricultural origin and modern cropland.

(B) Distributions of the Huai River Valley, and four cultural regions in and around the Huai River Valley (that is, the Zhongyuan Culture Region in northwest, the Haidai Culture Region in northeast, the Jianghan Culture Region in southwest, and the Jiangzhe Culture Region in southeast), isohyets, main river systems, mixed agriculture boundaries, and modern cities are also shown.

(C) Distributions of archaeological sites with the remains of the seeds of crop plants, elevation, and four cultural groups developed inside the Huai River Valley (that is, NW, NE, AH and SE).

(D) Distribution of archaeological settlement sites in the Huai River Valley.

Current quantitative Holocene cropland reconstructions typically rely on the extrapolation of historical population data and modern land use patterns during the prehistoric period (e.g., HYDE, History Database of the Global Environment).[26] By contrast, the reconstructions of GLUE (Global Land Use and Technological Evolution Simulator) use a simulated population based on the theoretical balance between population growth and regional cultural traits.[27,28] However, these studies all lack direct evidence for prehistoric human activity, and uncertainties persist in their reconstructions of cropland type, area, and distribution in the deep past.[29]

In recent years, the utility of incorporating archaeological data into prehistoric human land use reconstructions has become more widely recognized, with such data providing direct evidence of prehistoric human activity, including its type, intensity, and distribution.[29] One such approach, the prehistoric land use model (PLUM), has been successfully developed and applied in typical dry and rice cultivation areas in China,[30–32] providing a new tool to quantitatively reconstruct spatiotemporal changes in cropland areas over long timescales using archaeological data. The number and size of archaeological sites, and cultural parameters related to cultivation, have been used to improve the accuracy of cropland area reconstructions; and the relationship between the distributions of archaeological sites and environmental variables has been adopted to reconstruct the spatial patterns of cropland. Archaeological sites as control points can more accurately reflect the temporal fluctuations and spatial migration of prehistoric human activity.

The present study draws on PLUM and focuses on the Huai River Valley, the earliest and core area of mixed cropping in China.[9–11,33,34] During the Neolithic and Bronze Age (~10–2 ka BP), the valley was characterized by dry cultivation represented by *Setaria italica* and *Panicum miliaceum* (two types of millet) with lower water requirements, and rice cultivation represented by *Oryza sativa* with higher water requirements.[12] As noted, this valley is located in a transitional climatic zone, and it is also a zone of overlap between four key cultural regions (Figure 1B; more information about the valley is given in STAR Methods).[12,35] Four cultural groups correspondingly developed inside different parts of the Huai River Valley during the Neolithic Age (~10–4 ka BP) (Figure 1C): a group (NW) distributed in the northwest valley was mainly related to the Zhongyuan Cultural Region; a group (NE) distributed in the northeast valley was mainly related to the Haidai Cultural Region; a group (AH) distributed in the central and southern parts of the valley (mainly in Anhui province) was affected by all four cultural regions around; and a group (SE) distributed in the southeast valley was mainly related to the Jiangzhe Cultural Region

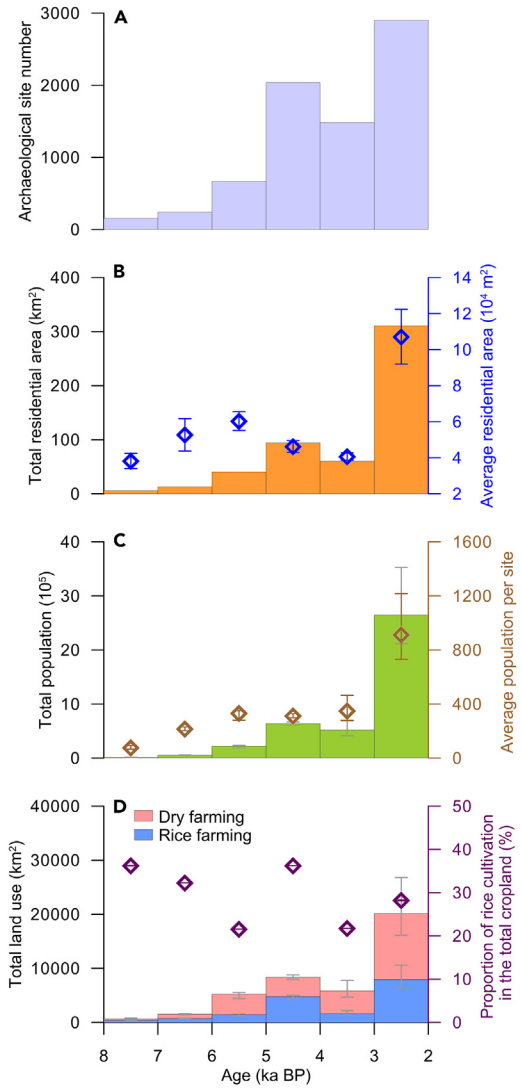

Figure 2. Temporal changes in human activity in the Huai River Valley

(A) Number of archaeological sites.

(B) Total and average residential areas (data are represented as average ± SEM).

(C) Total and average population (data are represented as minimum, average, and maximum values).

(D) Total cropland and proportion of rice cultivation in the total cropland (data are represented as minimum, average, and maximum values).

(Figures 1B and 1C).[14] Numerous Neolithic and Bronze Age archaeological sites have been found in the valley (Figures 1C, 1D, and S1).[36–40] The Huai River Valley is thus an ideal region for investigating the relative influences of climatic and cultural factors on the evolution of both cropland types and areas.

First, the different cropland types within the mixed cropping system need to be clarified in this study, hence, we first refined PLUM to PLUM2 by adding a new land use type sub-model based on crop seed floatation data from archaeological sites (Figures 1C and S2; more information is given in STAR Methods). Second, the distributions of cropland type and area (0.1° × 0.1° spatial resolution) in the Huai River Valley from 8 to 2 ka BP were quantitatively reconstructed based on archaeological and environmental data (Tables S2, S3, and S4), using PLUM2. Third, the corresponding spatial grid data of climatic and cultural factors in the valley were reconstructed based on pollen records (Table S5) and archaeological sites. The modern analog technique was adopted to produce quantitative reconstructions of annual mean temperature and precipitation, and the kernel density estimation (KDE) of archaeological sites was applied to illustrate the intensity of the distribution of different cultures (herein defined as cultural intensity). Finally, the relative contributions of climatic and cultural factors to cropland types and areal distributions from 8 to 2 ka BP in the valley were determined using multiple regression analysis, based on the reconstructed spatial grids of cropland, climatic factors, and cultural density.

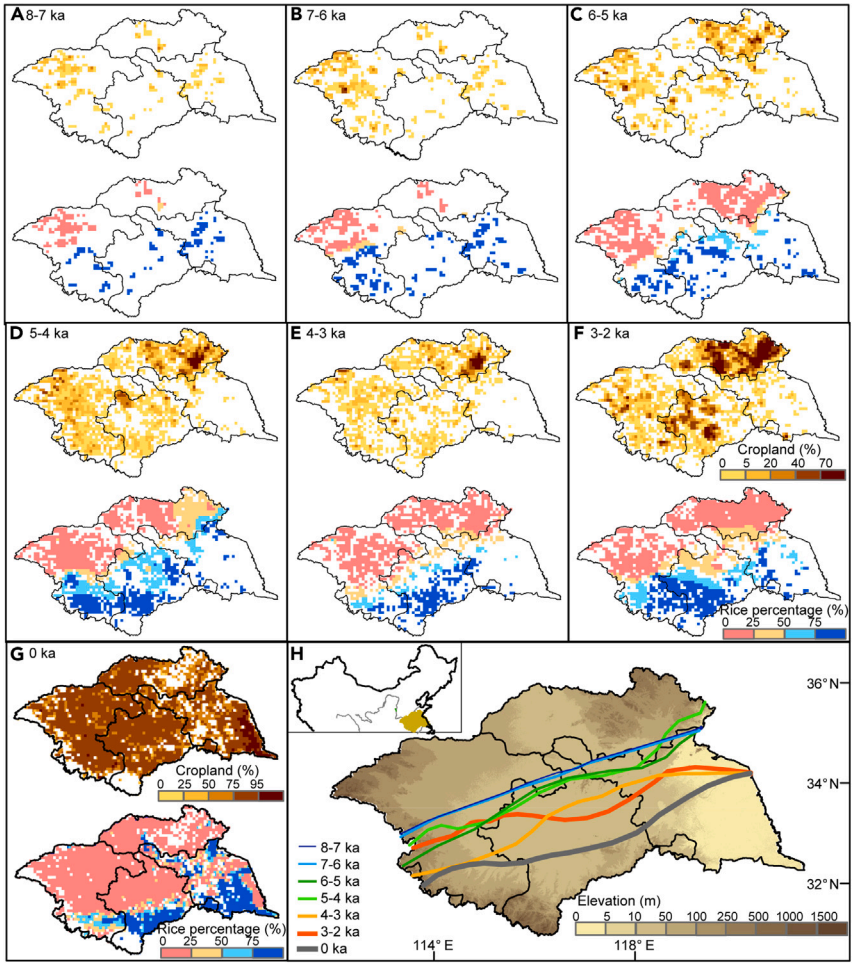

Figure 3. Spatial changes in cropland area and type, and in the northern boundaries of rice-dominated cropland (>50%)

Distributions of cropland type and area in the Huai River Valley during 8-7 ka BP (A), 7-6 ka BP (B), 6-5 ka BP (C), 5-4 ka BP (D), 4-3 ka BP (E), 3-2 ka BP (F), and 0 ka BP (G). Distributions of northern boundaries of rice-dominated cropland in the Huai River Valley from 8 to 0 ka BP (H).

RESULTS

Spatiotemporal changes in cropland type and area

Our results indicate that the number of archaeological sites in the Huai River Valley increased from 154 to 2,899 during 8–2 ka BP (Figures 2 and S1), and that the human population expanded from 1.2 (1.0–1.4)×10^4 individuals at 8–7 ka BP to 2.6 (2.1–3.5)×10^6 individuals at 3–2 ka BP, representing a total population increase by a factor of more than 200. Additionally, the cropland area expanded from 0.1 (0.08–0.12)×10^4 km^2 at 8–7 ka BP to 2.8 (2.2–3.7)×10^4 km^2 at 3–2 ka BP, representing a smaller increase, by a factor of 25. Intervals of significantly increased site numbers, population size, and cropland area occurred at 5–4 ka BP and 3–2 ka BP, while a temporary decrease in all of these variables occurred during 4–3 ka BP. However, the growth rate of both population and cropland area during the time window of 3–2 ka BP was much greater than the increase in the number of archaeological sites over the same period. This reflects a more substantial increase in the average and total residential areas of archaeological sites in the Huai River Valley compared to previous millennia (Figure 2).

Changes in dry and rice cultivated land use followed the same pattern as that of total cropland from 8 to 2 ka BP. The area of land under dry cultivation was always larger than that under rice cultivation over this period (Figure 2), but its spatial distribution was limited to the northern part of the valley before 6 ka BP, when rice cultivation was widely distributed across the entire valley (Figure S3). Therefore, the proportion of rice cultivation to total cropland area reached nearly 40% prior to 6 ka BP, but it decreased to <30% during 6–5 ka BP, with the southward expansion of dry cultivation. However, a pronounced increase in the proportion of rice cultivation to total cropland area occurred during 5–4 ka BP, while there was a decrease after 4 ka BP (Figure 2).

With the transformation of the distribution of archaeological sites in the Huai River Valley from scattered to extensive (Figure S1), three stages of cropland distribution can be distinguished (Figures 3 and S3). Prior to 6 ka BP, the total cropland area was mainly distributed around

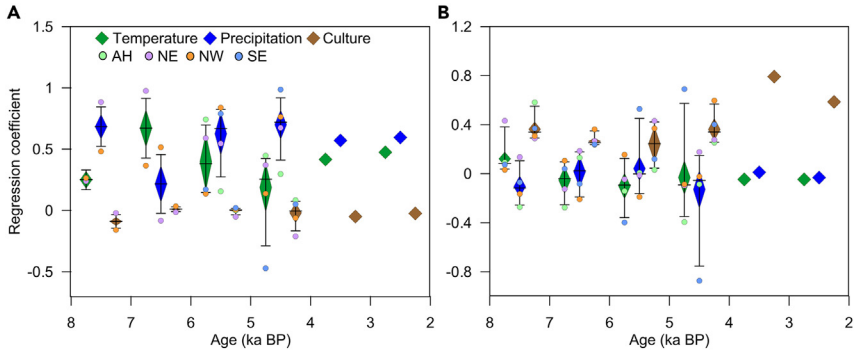

Figure 4. Changes in the contribution of different climatic and cultural factors to distribution of cropland

Cropland type (A) and area (B), the regression coefficients are represented as the mean and the values located at the 10%, 25%, 75%, and 90% positions of the data.

archaeological sites in the western, southern, and northeastern parts of the valley. The northern boundary of rice-dominated cropland (>50%) was located around 34°N. From 6 to 4 ka BP, the total cropland area expanded across the valley, except in its southeastern part. The increase in cropland area in the northern part of the valley was mainly the result of the intensification of dry cultivation during 6–5 ka BP, when dry and dry-dominated cropland began to expand southward. However, the expansion of both dry and rice cultivated land was substantial during 5–4 ka BP, as the northern boundary of the rice-dominated cropland area shifted to the north of 35°N in the eastern side of valley. After 4 ka BP, another cropland center developed in the central southern valley at 3–2 ka BP. The southward expansion of dry-dominated cropland was substantial, and its southern boundary shifted to the area around 33°N.

While 72% of the Huai River Valley area is under cultivation today (https://www.geodata.cn/) (Figure 3), in the period prior to 2 ka BP, less than 12% (8–14%) of the valley supported cropland, highlighting the relatively low intensity of prehistoric land use throughout most of the Holocene. However, after 5–4 ka BP, the distribution of cropland expanded to the entire valley (Figure 3), highlighting the human alteration of the regional land cover during the middle–late Holocene.

Main drivers of changes in cropland type and area distributions

The spatial grid data of climatic factors, cultural intensity, and cropland area were used for multiple regression analysis to determine the relative roles of climatic and cultural factors in the distribution of cropland type and area in the Huai River Valley from 8 to 2 ka BP (see STAR Methods). The dependent variables are the distributions of cropland type and area, the former represented by the proportion of rice cultivation to total cropland, and the latter by the proportion of total cropland relative to the entire valley area. The independent variables are the distributions of annual mean temperature (MAT), mean annual precipitation (MAP), and cultural intensity (Figures S4 and S5). Here, the kernel density distribution of archaeological sites from the four different cultural groups (that is, NW, NE, AH, and SE), which were related to the Zhongyuan, Haidai, Jianghan, and Jiangzhe culture regions (Figures 1B and 1C), reflects the spatial pattern and differences in the intensity of these cultural groups in the Huai River Valley (Figure S5).

The spatial distributions of reconstructed MAT and MAP during 8–2 ka BP all follow a decreasing trend from south to north in the Huai River Valley (Figure S4). The ranges of MAT and MAP across the valley are around 9.4°C–16.3°C and 738–1862 mm, respectively. The distributions of reconstructed cultural intensity demonstrate the evolutionary process from isolation, overlap, to integration, for these four cultural groups; these changes were mainly driven by the diffusion of the Yangshao, Dawenkou, Longshan cultures, and other local cultural types (Figure S5).

The multiple regression analysis results reveal that climatic factors played a key role in shaping the distribution of cropland type from 8 to 2 ka BP in the Huai River Valley, as the average regression coefficients of MAT and MAP were always greater that of cultural intensity (Figure 4A). Prior to 6 ka BP, the relative importance of temperature and precipitation varied through time (precipitation was more important during 8–7 ka BP, while temperature was more important during 7–6 ka BP), due to their varying contributions to the distribution of cropland types among the different cultural groups. However, the importance of precipitation increased after 6 ka BP, showing a consistently greater contribution to the distribution of cropland types among the different cultural groups.

By contrast, our results show that cultural intensity was the main driver of changes in the distribution of the cropland area in the Huai River Valley from 8 to 2 ka BP, since the average regression coefficients of cultural intensity were always greater than those of temperature and precipitation for this period (Figure 4B). Larger differences in average regression coefficients between cultural intensity and climatic factors after 4 ka BP indicate that the importance of cultural intensity had become even greater.

DISCUSSION

We have quantitatively reconstructed the spatiotemporal changes in cropland type and area from 8 to 2 ka BP in the Huai River Valley, a typical mixed cropping region in eastern China. Combined with the spatial patterns of climate, cultural intensity, and cropland data, multiple

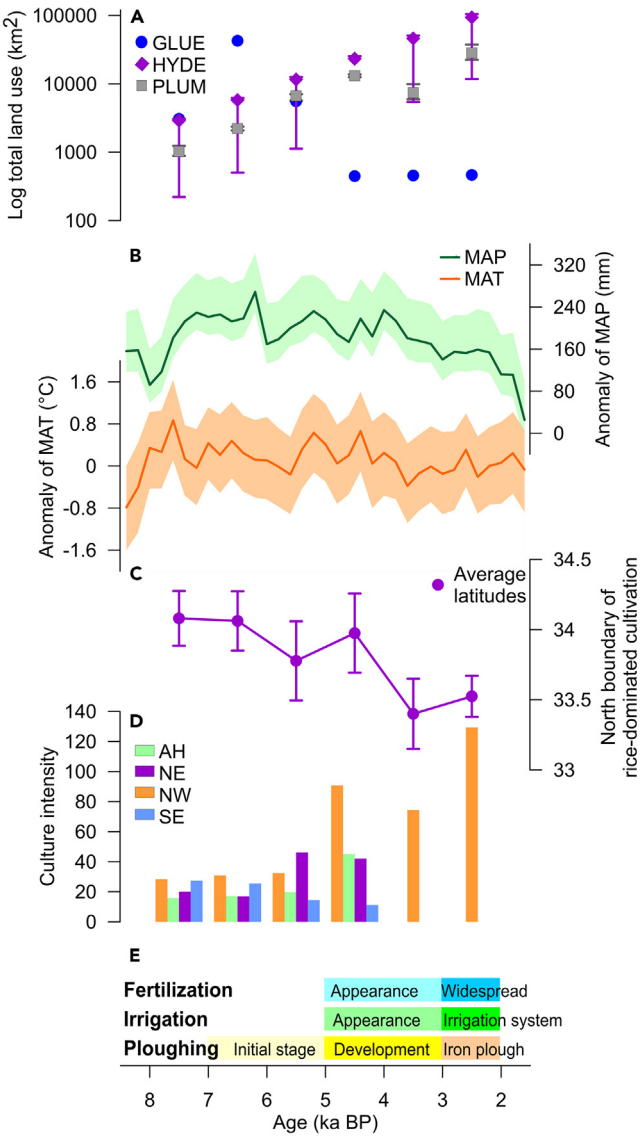

Figure 5. Comparison between temporal changes in cropland, climatic and cultural factors during 8-2 ka BP

(A) The cropland areas in the Huai River Valley reconstructed by different studies,[26,28] data are represented as minimum, average and maximum values.

(B) The reconstructed anomalies of MAT and MAP relative to present values based on pollen records in and around the valley, data are represented as the average and shading indicates 95% uncertainty bands of reconstructions.

(C) The northern boundary of rice-dominated cropland in the valley, data are represented as minimum, average and maximum values.

(D) Cultural intensity in the valley.

(E) Agricultural development in China.[41]

regression analysis was used to assess the relative roles of climatic and cultural factors in determining the changes in cropland type and area distributions through time.

Our results show an overall trend of cropland expansion from 8 to 2 ka BP, which is consistent with the results of HYDE3.2 (Figure 5A).[26] However, our results differ from those of GLUE,[28] which indicated that the area of cropland sharply increased at 7–6 ka BP, while the cropland areas were much lower than those estimated by PLUM and HYDE3.2 in the other periods (Figure 5A). The results of GLUE are clearly inaccurate for the Huai River Valley, which is likely the result of uncertainty in GLUE's population simulation and the relatively low resolution of its spatial reconstruction (0.5° × 0.5°).[28] The comparison of PLUM and HYDE3.2 shows that cropland expansion in HYDE3.2 was continuous, while that in PLUM shows a temporary decrease during 4–3 ka BP, leading to greater differences between their results after 4 ka BP (Figure 5A). From a spatial perspective, the distribution of cropland in HYDE3.2 indicated a significant dependence on the fluvial system, which also occurred during the recent period (Figure S6). By contrast, our reconstruction using PLUM reflects a distribution pattern centered around past human

settlements, with a preference for favorable environmental conditions such as low relative elevation, and slope, and closer proximity to rivers, which is likely a more accurate reflection of the past situation.

The most significant improvement of PLUM is the adoption of archaeological sites as control points for cropland reconstruction. The reconstructed distributions of cropland types based on floating results of carbonized crop seeds, consider the influences of climate fluctuations and cultural communications on cultivation over time. The reconstructed cropland areas and their distributions based on the number, size and distribution of archaeological sites, consider local differences in population size and land use efficiency, and large-scale human migration over time. Overall, these direct prehistoric human evidences more reliably reflect the temporal fluctuations and spatial variations of population and cropland, compared to the extrapolations of historical and modern human activity information in the previous studies.[26–28] For example, the decreasing values of land use per capita in PLUM (from 9.58 to 1.01 ha/capita during 8–2 ka BP) based on archaeological record of typical sites are broadly supported by the theoretical studies,[42–47] while the corresponding increasing values in HYDE3.2 (from 0.15 to 1.83 ha/capita during 8–2 ka BP) cannot be explained by the enhancing land use efficiency over time caused by population growth pressure and agricultural development.[26]

The distribution of cropland types in the Huai River Valley was directly controlled by the climatic conditions, since different crop plant species and varieties have specific temperature and precipitation ranges.[48,49] The reconstructed temperature and precipitation across the Huai River Valley during 8–2 ka BP were 9.4°C–16.3°C and 738–1,862 mm) (Figure S4), which were continuously within the ranges suitable for the growth of millet (5°C–45°C and 200–4,000 mm) and rice (10°C–36°C and 750–4,000 mm).[49] Accordingly, mixed crop agriculture was conducted in the Huai River Valley, showing a pattern of northern, millet-dominated cultivation with reduced heat and moisture requirements, and southern, rice-dominated cultivation requiring greater heat and moisture. However, the valley has distributed in the edge regions of both millet and rice cultivations, as at present only parts of the valley fall into the precipitation optimum ranges for two types of cultivation (millet 500–750 mm and rice 1,000–2,000 mm), while the entire valley does not fall into the temperature optimum ranges (millet 16°C–32°C, rice 20°C–30°C) (Figures S4M and S4N). From 8 to 2 ka BP, the precipitation optimum areas for rice cultivation enlarged obviously in the valley, while the optimum areas for millet cultivation almost disappeared. By the contrast, a small temperature optimum area for millet cultivation appeared in the southwestern valley during 8–4 ka BP, while there was still no temperature optimum area for rice cultivation (Figures S4A–S4L). Therefore, the distribution of rice-dominated cultivation was most sensitive to changes in precipitation inside the valley during 8–2 ka BP, which explains the results revealed by regression analysis that the distribution of cropland types was mainly controlled by precipitation (Figure 4A). The comparison of time series evolutions further reveal the synchronous changes between rice-dominated cultivation boundary and climatic factors during 8–2 ka BP (Figures 5B and 5C). The southward retreats of rice-dominated cultivation during 6–5 ka BP and 4–3 ka BP corresponded to the decreases of temperature and precipitation, while the northward expansion of rice-dominated cultivation during 5–4 ka BP synchronized with the increases of the climatic factors. As climate change only fluctuated within a small range during 8–4 ka BP, the shifts of rice-dominated cultivation boundary during the period were less significant than that during 4–3 ka BP (Figures 3B and 3C).

Regarding the dominant role of cultural intensity in determining the distribution of cropland areas in the Huai River Valley, the balance between the population food demand and the cropland food supply was the key factor linking culture and land use. Prior to 4 ka BP, the differences between the contributions of cultural intensity and climatic factors to the distribution of cropland area were less significant (Figure 4B), since a warm and wet climate favored continuous cultural development (Figure 5B), and also played a positive role in the growth of population and cropland area in the valley. However, the contradictory changes evidenced by the worsening climate conditions and the growth of the human population and cropland during 3–2 ka BP confirms the influence of cultural development on the distribution of cropland area, with cultural developments surpassing the effects of climate change. Arguably this was because societal resilience was enhanced due the establishment of a nation state, the diversification of cultivation,[50] and continuous advances in agricultural technology (e.g., the development of iron tools, irrigation, and fertilization application) (Figure 5D).[41] As for the abnormal decrease of cropland area across the valley during 4–3 ka BP, it was sync with the widespread cultural decline in eastern China. Besides the contribution of climate change,[51] flooding was another potential factor causing the decline of Neolithic culture around 4 ka BP and the following decrease of cropland area in the valley, which was also supported by regional geological records.[52]

Above all, the responses of cropland size and types to changes in climatic and cultural factors in the Huai River Valley revealed here support the previous records comparison studies about the correlations between climate evolution, culture development, agriculture dispersal, population fluctuation and migration,[12,53–59] as most of the studies attributed the rice cultivation expansion and population growth during the middle Holocene to favorable climate conditions. However, these previous studies mainly qualitatively explored the impact of climate and cultural factors on population size/cropland area at temporal scales. Here, our cognition of the dominant factors in the spatial evolution of population/cropland has improved, as the approach adopted in this study for controlling factor analysis begins from the perspective of the spatial pattern of cropland, and the reconstructed spatially continuous cropland distribution enables a semi-quantitative and quantitative analysis of the factors controlling both cropland types and their areal distributions. It thus provides a more comprehensive understanding of the relationship between climate, culture, and cropland evolution, providing support for the development of dynamic land use models and future land use predictions.

Studying the relationship among changes in population, cropland, culture, and climate during the warm and humid climate of the Holocene provides important historical reference points for assessing the impacts of present and future global warming.[60,61] Our research confirms that in the face of increasing population pressure, humans in mixed cropping areas can adapt to climate change by modifying the spatial distribution of regional crop cultivation. Historically informed and strategic planning of crop production adaptations in mixed cropping areas can help support community resilience in an era of ongoing and increasing climate challenges.

Limitations of the study

The current reconstruction based on recorded archaeological sites only provides lower limits on actual prehistoric populations and cropland areas, due to the effects of fluvial erosion, human disturbance, and other taphonomic factors on site preservation, especially for earlier millennia.[36–39]

Since PLUM is based on the assumptions of a single land use type (cropland) and a closed balance of food needs and supply in this region, more accurate land use per-capita estimates can be obtained by improving the structure of PLUM by incorporating other human activities (e.g., hunting, gathering, grazing, and livestock feeding) related to land use in a future version of the model.

RESOURCE AVAILABILITY

Lead contact

Requests for further information and resources should be directed to the lead contact, Yu Yanyan (yyy@mail.iggcas.ac.cn).

Materials availability

This study did not generate new materials.

Data and code availability

- Data reported in this paper will be shared by the lead contact upon reasonable request.
- This paper does not report original code.
- Any additional information required to reanalyze the data reported in this paper is available from the lead contact upon request.

ACKNOWLEDGMENTS

This work was funded by the Global Change Program of National Key Research and Development Program of China (no. 2020YFA0607703) and the National Natural Science Foundation of China (no. T2192954, no. 42488201, no. 41888101, and no. 42177180).

AUTHOR CONTRIBUTIONS

Conceptualization, Y.Y. and H.W.; methodology, Y.Y. and J.Y.; data curation, W.Z. and J.Y.; formal analysis, Y.Y., W.Z., and J.Y.; writing – original draft, Y.Y. and H.W.; writing – review & editing, Y.Y., H.W., N.B., J.Z., X.Z., W.L., C.D., J.G., and Z.G.; funding acquisition, Y.Y. and Z.G.

DECLARATION OF INTERESTS

The authors declare no competing interests.

STAR★METHODS

Detailed methods are provided in the online version of this paper and include the following:

- KEY RESOURCES TABLE
- EXPERIMENTAL MODEL AND STUDY PARTICIPANT DETAILS
- METHOD DETAILS
  - Study region and interval
  - Archaeological and pollen datasets
  - PLUM model and improvements
  - Paleoclimate reconstruction
  - Reconstructing cultural intensity
  - Multiple regression analysis of climatic and cultural factors
- QUANTIFICATION AND STATISTICAL ANALYSIS

SUPPLEMENTAL INFORMATION

Supplemental information can be found online at https://doi.org/10.1016/j.isci.2024.110841.

Received: March 16, 2024
Revised: July 20, 2024
Accepted: August 26, 2024
Published: September 5, 2024

REFERENCES

1. Kastner, T., Rivas, M.J.I., Koch, W., and Nonhebel, S. (2012). Global changes in diets and the consequences for land requirements for food. Proc. Natl. Acad. Sci. USA *109*, 6868–6872.
2. Lizarazo, C.I., Tuulos, A., Jokela, V., and Mäkelä, P.S.A. (2020). Sustainable mixed cropping systems for the Boreal-Nemoral region. Front. Sustain. Food Syst. *4*, 103.
3. Gliessman, S.R. (1985). Multiple cropping systems: a basis for developing an alternative agriculture. In U.S. Congress, Office of Technology Assessment ed. Innovative Biological Technologies for Lesser Developed Countries-Workshop Proceedings (U.S. Government Printing Office), pp. 69–83.
4. Li, H., Liu, Z., James, N., Li, X., Hu, Z., Shi, H., Sun, L., Lu, Y., and Jia, X. (2021). Agricultural transformations and their influential factors revealed by archaeobotanical evidence in

Holocene Jiangsu Province, Eastern China. Front. Earth Sci. *9*, 661–684.
5. Yang, H., Zhang, W.P., and Li, L. (2021). Intercropping feed more people and build more sustainable agroecosystems. Front. Agr. Sci. Eng. *8*, 373–386.
6. Waha, K., Dietrich, J.P., Portmann, F.T., Siebert, S., Thornton, P.K., Bondeau, A., and Herrero, M. (2020). Multiple cropping systems of the world and the potential for increasing cropping intensity. Glob. Environ. Change *64*, 102131.
7. Potapov, P., Turubanova, S., Hansen, M.C., Tyukavina, A., Zalles, V., Khan, A., Song, X.P., Pickens, A., Shen, Q., and Cortez, J. (2022). Global maps of cropland extent and change show accelerated cropland expansion in the twenty-first century. Nat. Food *3*, 19–28.
8. Bellwood, P. (2005). First Farmers: The Origins of Agricultural Societies (Blackwell), pp. 12–43.
9. Zhang, J., Lu, H., Gu, W., Wu, N., Zhou, K., Hu, Y., Xin, Y., and Wang, C. (2012). Early mixed farming of millet and rice 7800 years ago in the middle Yellow River Region, China. PLoS One *7*, e52146.
10. Wang, C., Lu, H., Gu, W., Zuo, X., Zhang, J., Liu, Y., Bao, Y., and Hu, Y. (2018). Temporal changes of mixed millet and rice agriculture in Neolithic-Bronze Age Central Plain, China: archaeobotanical evidence from the Zhuzhai site. Holocene *28*, 738–754.
11. Bestel, S., Bao, Y., Zhong, H., Chen, X., and Liu, L. (2017). Wild plant use and multi-cropping at the early Neolithic Zhuzhai site in the middle Yellow River region, China. Holocene *28*, 195–207.
12. He, K., Lu, H., Zhang, J., Wang, C., and Huan, X. (2017). Prehistoric evolution of the dualistic structure mixed rice and millet farming in China. Holocene *27*, 1885–1898.
13. Yang, Y., Yang, M., Sun, B., Li, W., Cheng, Z., Yao, L., Lan, W., Zhou, X., and Zhang, J. (2023). Mixed farming of rice and millets became the primary subsistence strategy 6400 years ago in the western Huanghuai Plain of Central China: new macrofossil evidence from Shigu. Archaeol. Anthropol. Sci. *15*, 122.
14. Yan, W.M. (1997). The cradle of oriental civilization. In The Origins of Agriculture and the Rise of Civilization, W.M. Yan, ed. (Sciences Press), pp. 148–174.
15. Gronenborn, D. (2009). Climate fluctuations and trajectories to complexity in the Neolithic: towards a theory. Doc. Praeh. *36*, 97–110.
16. Leipe, C., Long, T., Sergusheva, E.A., Wagner, M., and Tarasov, P.E. (2019). Discontinuous spread of millet agriculture in eastern Asia and prehistoric population dynamics. Sci. Adv. *5*, eaax6225.
17. Aneli, S., Mezzavilla, M., Bortolini, E., Pirastu, N., Girotto, G., Spedicati, B., Berchialla, P., Gasparini, P., and Pagani, L. (2022). Impact of cultural and genetic structure on food choices along the Silk Road. Proc. Natl. Acad. Sci. USA *119*, e2209311119.
18. Hosner, D., Wagner, M., Tarasov, P.E., Chen, X., and Leipe, C. (2016). Spatiotemporal distribution patterns of archaeological sites in China during the Neolithic and Bronze Age: an overview. Holocene *26*, 1576–1593.
19. Bevan, A., Colledge, S., Fuller, D., Fyfe, R., Shennan, S., and Stevens, C. (2017). Holocene fluctuations in human population demonstrate repeated links to food production and climate. Proc. Natl. Acad. Sci. USA *114*, E10524–E10531.
20. Warden, L., Moros, M., Neumann, T., Shennan, S., Timpson, A., Manning, K., Sollai, M., Wacker, L., Perner, K., Häusler, K., et al. (2017). Climate induced human demographic and cultural change in northern Europe during the mid-Holocene. Sci. Rep. *7*, 15251.
21. Islebe, G.A., Torrescano-Valle, N., Valdez-Hernández, M., Carrillo-Bastos, A., and Aragón-Moreno, A.A. (2022). Maize and ancient Maya droughts. Sci. Rep. *12*, 22272.
22. He, K., Lu, H., Jin, G., Wang, C., Zhang, H., Zhang, J., Xu, D., Shen, C., Wu, N., and Guo, Z. (2022). Antipodal pattern of millet and rice demography in response to 4.2 ka climate event in China. Quat. Sci. Rev. *295*, 107786.
23. Kennett, D.J., Lipson, M., Prufer, K.M., Mora-Marín, D., George, R.J., Rohland, N., Robinson, M., Trask, W.R., Edgar, H.H.J., Hill, E.C., et al. (2022). South-to-north migration preceded the advent of intensive farming in the Maya region. Nat. Commun. *13*, 1530. https://doi.org/10.1038/s41467-022-29158-y.
24. He, K., Lu, H., Zhang, J., and Wang, C. (2022). Holocene spatiotemporal millet agricultural patterns in northern China: a dataset of archaeobotanical macroremains. Earth Syst. Sci. Data *14*, 4777–4791. https://doi.org/10.5194/essd-14-4777-2022.
25. Li, R., Lv, F., Yang, L., Liu, F., Liu, R., and Dong, G. (2020). Spatial-temporal variation of cropping patterns in relation to climate change in Neolithic China. Atmosphere *11*, 677.
26. Klein Goldewijk, K., Beusen, A., Doelman, J., and Stehfest, E. (2017). Anthropogenic land use estimates for the Holocene - HYDE 3.2. Earth Syst. Sci. Data *9*, 927–953.
27. Kaplan, J.O., Krumhardt, K.M., Ellis, E.C., Ruddiman, W.F., Lemmen, C., and Goldewijk, K.K. (2011). Holocene carbon emissions as a result of anthropogenic land cover change. Holocene *21*, 775–791.
28. Lemmen, C. (2009). World distribution of land cover changes during pre- and protohistoric times and estimation of induced carbon releases. Géomorphologie *15*, 303–312.
29. ArchaeoGLOBE Project (2019). Archaeological assessment reveals Earth's early transformation through land use. Science *365*, 897–902.
30. Yu, Y., Guo, Z., Wu, H., and Finke, P.A. (2012). Reconstructing prehistoric land use change from archeological data: validation and application of a new model in Yiluo valley, northern China. Agric. Ecosyst. Environ. *156*, 99–107.
31. Yu, Y., Wu, H., Finke, P.A., and Guo, Z. (2016). Spatial and temporal changes of prehistoric human land use in the Wei River valley, northern China. Holocene *26*, 1788–1801.
32. Yu, J., Yu, Y., Wu, H., Zhang, W., and Liu, H. (2022). Spatiotemporal changes in early human land use during the Holocene throughout the Yangtze River Basin, China. Holocene *32*, 334–345.
33. Zhang, J.Z. (2005). A brief discussion of Neolithic culture in the Huai River area. J Zhengzhou Univ *38*, 7–10.
34. Luo, W., Gu, C., Yang, Y., Zhang, D., Liang, Z., Li, J., Huang, C., and Zhang, J. (2019). Phytoliths reveal the earliest interplay of rice and broomcorn millet at the site of Shuangdun (ca. 7.3–6.8 ka BP) in the middle Huai River valley, China. J. Archaeol. Sci. *102*, 26–34.
35. Liu, L., and Chen, X.C. (2017). The Archaeology of China: From the Late Paleolithic to the Early Bronze Age (SDX Joint Publishing Company), pp. 50–482.
36. National Heritage Board (1991). Atlas of Chinese Cultural Relics: Henan Branch (Sino Maps Press), pp. 1–576.
37. National Heritage Board (2007). Atlas of Chinese Cultural Relics: Shandong Branch (Sino Maps Press), pp. 1–912.
38. National Heritage Board (2008). Atlas of Chinese Cultural Relics: Jiangsu Branch (Sino Maps Press), pp. 1–777.
39. National Heritage, Board. (2014). Atlas of Chinese Cultural Relics: Anhui Branch (Sino Maps Press), pp. 1–535.
40. National Heritage Board (2002). Atlas of Chinese Cultural Relics: Hubei Branch (Xi'an Map Publishing House), pp. 1–606.
41. Su, L. (2008). Characteristics Analysis of Chinese Traditional Agricultural Technology Evolution (Northeastern University), pp. 16–24.
42. Wang, J.G. (1997). Population, ecology and evolution of China's slash and burn areas. Agr. Archaeol. *1*, 152.
43. Wang, J.H. (2011). Study on the Prehistoric Population in the Middle and Lower Reaches of the Yellow River (Science Press), pp. 25–178.
44. Boserup, E. (1981). Population and Technological Change: A Study of Long Term Trends (University of Chicago Press), pp. 3–92.
45. Johnston, K.J. (2003). The intensification of pre-industrial cereal agriculture in the tropics: Boserup, cultivation lengthening, and the Classic Maya. J. Anthropol. Archaeol. *22*, 126–161.
46. Kaplan, J.O., Krumhardt, K.M., and Zimmermann, N. (2009). The prehistoric and preindustrial deforestation of Europe. Quat. Sci. Rev. *28*, 3016–3034.
47. Ruddiman, W.F., and Ellis, E.C. (2009). Effect of per-capita land use changes on Holocene forest clearance and CO_2 emissions. Quat. Sci. Rev. *28*, 3011–3015.
48. Bao, Y., Zhou, X., Liu, H., Hu, S., Zhao, K., Atahan, P., Dodson, J., and Li, X. (2018). Evolution of prehistoric dryland agriculture in the arid and semi-arid transition zone in northern China. PLoS One *13*, e0198750.
49. Zhou, X.Y., Lin, Z., Spengler, R.N., Zhao, K.L., Liu, J.C., Xu, X., Bao, Y.G., Dodson, J., Xu, H., and Li, X.Q. (2020). Water management and wheat yields in ancient China: carbon isotope discrimination of archaeological wheat grains. Holocene *31*, 285–293.
50. Ren, X., Xu, J., Wang, H., Storozum, M., Lu, P., Mo, D., Li, T., Xiong, J., and Kidder, T.R. (2021). Holocene fluctuations in vegetation and human population demonstrate social resilience in the prehistory of the Central Plains of China. Environ. Res. Lett. *16*, 055030.
51. Wu, W.X., and Liu, T.S. (2004). Possible role of the Holocene Event 3 on the collapse of Neolithic Cultures around the Central Plain of China. Quat. Int. *117*, 153–166.
52. Zhang, G.S., Zhu, C., Wang, J.H., Zhu, G.Y., Ma, C.M., Zheng, C.G., Zhao, L.H., Li, Z.X., Zhu, Q., and Jin, A.C. (2009). Environmental archaeology of Longshan culture period on Yuhuicun site from 4.5 ka to 4.0 ka BP, Bengbu, Anhui. Acta Geog. Sin. *64*, 817–827.

53. Huang, X., Xiang, L., Lei, G., Sun, M., Qiu, M., Storozum, M., Huang, C., Munkhbayar, C., Demberel, O., Zhang, J., et al. (2021). Sedimentary Pediastrum record of middle-late Holocene temperature change and its impacts on early human culture in the desert-oasis area of northwestern China. Quat. Sci. Rev. *265*, 107054.
54. Xiang, L., Huang, X., Sun, M., Panizzo, V.N., Huang, C., Zheng, M., Chen, X., and Chen, F. (2023). Prehistoric population expansion in Central Asia promoted by the Altai Holocene Climatic Optimum. Nat. Commun. *14*, 3102.
55. Wang, C., Lv, H.Y., Gu, W.F., Wu, N.Q., Zhang, J.P., Zuo, X.X., Li, F.J., Wang, D.J., Dong, Y.J., Wang, S.Z., et al. (2019). Spatial-temporal evolution of agriculture and factors influencing it during the mid-Holocene in Zhengzhou area, China. Quat. Sci. *39*, 108–122.
56. Guo, R.Z. (2019). Archaeological Study of Prehistoric Agriculture in Haidai Region – Centered on Plant Remains (Shandong University), pp. 137–150.
57. Huang, R., Zhu, C., and Zheng, C.G. (2005). Distribution of Neolithic sites and environmental change in Huaihe River Basin, Anhui province. Acta Geog. Sin. *60*, 742–750.
58. Sun, W. (2010). The Relationship between the Cultural Channel of Neolithic Sites and the Geographical Environment in Anhui Province (Nanjing University), pp. 43–59.
59. Huang, K., Xie, D., Chen, C., Tang, Y., Wan, Q., and Zhang, X. (2023). An environmental crisis and its cultural impact in eastern China around 6000 years ago. Palaeogeogr. Palaeocl. *624*, 111652.
60. Rick, T.C., and Sandweiss, D.H. (2020). Archaeology, climate, and global change in the Age of Humans. Proc. Natl. Acad. Sci. USA *117*, 8250–8253.
61. Boivin, N., and Crowther, A. (2021). Mobilizing the past to shape a better Anthropocene. Nat. Ecol. Evol. *5*, 273–284.
62. Juggins, S. (2020). Rioja: analysis of Quaternary science data. https://cran.r-project.org/package=rioja.
63. Cao, Q., and Qi, Y. (2014). The variability of vertical structure of precipitation in Huaihe River Basin of China: implications from long-term spaceborne observations with TRMM precipitation radar. Water Resour. Res. *50*, 3690–3705.
64. Peng, B. (2016). Remains of early rice farming in China and related issues. Agr. Ecosyst. *1*, 40–45.
65. Chen, Z.Y., and Zhou, J.L. (2005). Xia, Shang, Zhou and the Huai River Basin. J Zhengzhou Univ *2*, 15–16. (Philosophy and Social Sciences Edition).
66. Expert Group on Xia Shang Zhou Chronology Engineering (2022). Report on the Xia Shang Zhou Chronology Project (Science Press), p. 517.
67. Ruddiman, W.F., Guo, Z., Zhou, X., Wu, H., and Yu, Y. (2008). Early rice farming and anomalous methane trends. Quat. Sci. Rev. *27*, 1291–1295.
68. Yu, Y.Y. (2010). Dynamics of Terrestrial Carbon Storage in China with Vegetation Evolution and Land Use Change during the Holocene (Institute of Geology and Geophysics, Chinese Academy of Sciences), pp. 56–64.
69. Silva, F., Stevens, C.J., Weisskopf, A., Castillo, C., Qin, L., Bevan, A., and Fuller, D.Q. (2015). Modelling the geographical origin of rice cultivation in Asia using the rice archaeological database. PLoS One *10*, e0137024.
70. Araus, J.L., Slafer, G.A., Buxó, R., and Romagosa, I. (2003). Productivity in prehistoric agriculture: physiological models for the quantification of cereal yields as an alternative to traditional approaches. J. Archaeol. Sci. *30*, 681–693.
71. Wu, R.K. (1995). Thoughts on the whole course of human evolution. Acta Anthropol. Sin. *14*, 285–296.
72. Zheng, Y.F., Sun, G.P., Qin, L., Li, C.H., Wu, X.H., and Chen, X.G. (2009). Rice fields and modes of rice cultivation between 5000 and 2500 BC in east China. J. Archaeol. Sci. *36*, 2609–2616.
73. Zheng, Y., Singarayer, J.S., Cheng, P., Yu, X., Liu, Z., Valdes, P.J., and Pancost, R.D. (2014). Holocene variations in peatland methane cycling associated with the Asian summer monsoon system. Nat. Commun. *5*, 4631.
74. Wu, H. (1985). Research on Grain Yield Per Mu in Chinese History (Agricultural Publishing House), pp. 100–141.
75. Gao, Z.Y., and Min, H.Y. (2008). A study on the changes of human land relations of the Dulong Ethnic Group in the 20th century. Frontline Thought *4*, 31–35.
76. Song, Z.L. (1982). The agriculture of the Mosuo People by the Lugu lake. Agr. Archaeol. *1*, 114–121. 196.
77. Guo, W.T. (1994). Research on the History of Chinese Farming System. (Hehai University Press), pp. 1–372.
78. Yang, Q.Y., Chen, Z.T., Xin, G.X., and Li, Z. (2018). The historical evolution of Chinese cultivation system and some thoughts on the current land fallow and crop rotation policy. West Forum *28*, 1–8.
79. Zheng, C.G., Zhu, C., Zhong, Y.S., Yin, P.L., Bai, J.J., and Sun, Z.B. (2008). The temporal and spatial distribution of archeological sites and natural environment from Paleolithic Age to Tang and Song Dynasties in reservoir region of Chongqing. Chin. Sci. Bull. *53*, 93–111.
80. Herzschuh, U., Cao, X., Laepple, T., Dallmeyer, A., Telford, R.J., Ni, J., Chen, F., Kong, Z., Liu, G., Liu, K.B., et al. (2019). Position and orientation of the westerly jet determined Holocene rainfall patterns in China. Nat. Commun. *10*, 2376.
81. Li, Q., Wu, H., Yu, Y., Sun, A., and Luo, Y. (2019). Large-scale vegetation history in China and its response to climate change since the Last Glacial Maximum. Quat. Int. *500*, 108–119.
82. Webb, T.I. (1985). A Global Paleoclimatic Data Base for 6000 Yr BP (Brown University, Department of Geological Sciences), pp. 25–34.
83. Reimer, P.J., Austin, W.E.N., Bard, E., Bayliss, A., Blackwell, P.G., Bronk Ramsey, C., Butzin, M., Cheng, H., Edwards, R.L., Friedrich, M., et al. (2020). The IntCal20 Northern Hemisphere radiocarbon age calibration curve (0–55 cal kBP). Radiocarbon *62*, 725–757.
84. Blaauw, M. (2010). Methods and code for 'classical' age-modelling of radiocarbon sequences. Quat. Geochronol. *5*, 512–518.
85. Giesecke, T., Davis, B., Brewer, S., Finsinger, W., Wolters, S., Blaauw, M., de Beaulieu, J.L., Binney, H., Fyfe, R.M., Gaillard, M.J., et al. (2014). Towards mapping the late Quaternary vegetation change of Europe. Veg. Hist. Archaeobot. *23*, 75–86.
86. Zheng, Z., Wei, J., Huang, K., Xu, Q., Lu, H., Tarasov, P., Luo, C., Beaudouin, C., Deng, Y., Pan, A., et al. (2014). East Asian pollen database: modern pollen distribution and its quantitative relationship with vegetation and climate. J. Biogeogr. *41*, 1819–1832.
87. Harris, I., Jones, P.D., Osborn, T.J., and Lister, D.H. (2014). Updated high-resolution grids of monthly climatic observations – the CRU TS3.10 Dataset. Int. J. Climatol. *34*, 623–642.
88. Zhang, W., Wu, H., Cheng, J., Geng, J., Li, Q., Sun, Y., Yu, Y., Lu, H., and Guo, Z. (2022). Holocene seasonal temperature evolution and spatial variability over the Northern Hemisphere landmass. Nat. Commun. *13*, 5334.
89. Overpeck, J.T., Webb, T., III, and Prentice, I.C. (1985). Quantitative interpretation of fossil pollen spectra: Dissimilarity coefficients and the method of modern analogs. Quat. Res. *23*, 87–108.
90. Simpson, G.L. (2012). Analogue methods in Palaeolimnology. In Tracking Environmental Change Using Lake Sediments, H.J.B. Birks, A.F. Lotter, S. Juggins, and J.P. Smol, eds. (Springer), pp. 495–522.
91. Peyron, O., Guiot, J., Cheddadi, R., Tarasov, P., Reille, M., de Beaulieu, J.-L., Bottema, S., and Andrieu, V. (1998). Climatic reconstruction in Europe for 18,000 yr B.P. from pollen data. Quat. Res. *49*, 183–196.
92. Davis, B.A.S., Brewer, S., Stevenson, A.C., and Guiot, J. (2003). The temperature of Europe during the Holocene reconstructed from pollen data. Quat. Sci. Rev. *22*, 1701–1716.
93. Prentice, I.C., Cramer, W., Harrison, S.P., Leemans, R., Monserud, R.A., and Solomon, A.M. (1992). A global biome model based on plant physiology and dominance, soil properties and climate. J. Biogeogr. *19*, 117–134.
94. Yu, G., Chen, X., Ni, J., Cheddadi, R., Guiot, J., Han, H., Harrison, S.P., Huang, C., Ke, M., Kong, Z., et al. (2000). Palaeovegetation of China: a pollen data-based synthesis for the mid-Holocene and last glacial maximum. J. Biogeogr. *27*, 635–664.
95. Williams, J.W., and Shuman, B. (2008). Obtaining accurate and precise environmental reconstructions from the modern analog technique and North American surface pollen dataset. Quat. Sci. Rev. *27*, 669–687.
96. Davis, B.A.S., Collins, P.M., and Kaplan, J.O. (2015). The age and post-glacial development of the modern European vegetation: a plant functional approach based on pollen data. Veg. Hist. Archaeobot. *24*, 303–317.
97. Marsicek, J., Shuman, B.N., Bartlein, P.J., Shafer, S.L., and Brewer, S. (2018). Reconciling divergent trends and millennial variations in Holocene temperatures. Nature *554*, 92–96.
98. Xu, H., Wang, T., Wang, H., Chen, S., and Chen, J. (2023). External forcings caused the tripole trend of Asian precipitation during the Holocene. JGR. Atmospheres *128*, e2023JD039460.
99. Cheng, X., and Shi, J. (2024). Simulation of the time-transgressive nature of East Asian summer monsoon precipitation over the Holocene. Quat. Sci. *44*, 593–604.
100. Zhang, X., Zheng, Z., Huang, K., Cheng, J., Cheddadi, R., Zhao, Y., Liang, C., Yang, X., Wan, Q., Tang, Y., et al. (2023). Quantification of Asian monsoon variability

from 68 ka BP through pollen-based climate reconstruction. Sci. Bull. *68*, 713–722.

101. Liu, W., Xue, Y., and Shang, C. (2023). Spatial distribution analysis and driving factors of traditional villages in Henan province: a comprehensive approach via geospatial techniques and statistical models. Herit. Sci. *11*, 185.

102. Zimmermann, A., Hilpert, J., and Wendt, K.P. (2009). Estimations of population density for selected periods between the Neolithic and AD 1800. Hum. Biol. *81*, 357–380.

103. Schmidt, I., Bradtmöller, M., Kehl, M., Pastoors, A., Tafelmaier, Y., Weninger, B., and Weniger, G.-C. (2012). Rapid climate change and variability of settlement patterns in Iberia during the Late Pleistocene. Quat. Int. *274*, 179–204.

104. Rubinfeld, D.L. (1994). Reference Guide on Multiple Regression. In Reference Manual on Scientific Evidence, Federal Judicial Center, ed. (U.S. Government Printing Office), pp. 415–469.

105. Kumar, M. (2016). Impact of climate change on crop yield and role of model for achieving food security. Environ. Monit. Assess. *188*, 465.

106. Castro, P.V., Chapman, R.W., Gili, S., Lull, V., Micó, R., Rihuete, C., Risch, R., and Sanahuja, M.E. (1999). Agricultural production and social change in the Bronze Age of southeast Spain: the Gatas project. Antiquity *73*, 846–856.

STAR★METHODS

KEY RESOURCES TABLE

REAGENT or RESOURCE	SOURCE	IDENTIFIER
Deposited data		
Elevation	Shuttle Radar Topography Mission (SRTM)	http://srtm.csi.cgiar.org/
Soil type	National Earth System Science Data Center	http://www.geodata.cn/
River system	National Earth System Science Data Center	http://www.geodata.cn/
Modern monthly mean temperature and precipitation	University of East Anglia Climatic Research Unit	https://crudata.uea.ac.uk/cru/data/hrg/
Software and algorithms		
R package 'Rioja'	Juggins[62]	https://cran.r-project.org/package=rioja.
ArcGIS10.2	GeoScene Information Technology Co Ltd	https://www.arcgis.com/
PASW Statistics18	SBAS Limited	http://www.spss.com.hk/statistics/

EXPERIMENTAL MODEL AND STUDY PARTICIPANT DETAILS

This study does not use experimental models.

METHOD DETAILS

Study region and interval

The Huai River Valley is located in eastern China (30.92°–36.60°N, 111.92°–121.42°E), comprising a total area of 2.7×10^5 km^2. The area lies in between the Yellow River Valley and the Yangtze River Valley. The topography of the valley is high in the west and low in the east, and around 2/3 of it comprises plains (Figure 1). The modern annual mean temperature in the valley is ~11–16°C, and the annual mean precipitation is ~910 mm.[63] The natural vegetation in the valley varies from alpine vegetation and subtropical mountainous cold temperate coniferous forest in the west, to subtropical evergreen broadleaved forest in the east (http://www.resdc.cn/). Currently, 72% of the area of the valley is cultivated (https://www.geodata.cn/). The dominant soil types are paddy soils (WRB: Anthrosols), yellow-brown soils (WRB: Cambisols), red soils, yellow soils (WRB: Cambisols), and purplish soils (WRB: Cambisols) (http://envi.ckcest.cn/environment/).

The time period addressed in the study is from ~8 to 2 ka BP (including the Neolithic Age and Bronze Age), as the earliest mixed cultivation found at Jiahu site in the Huai River Valley was dated to 8250 a BP,[64] and few archaeological sites younger than 2 ka BP have been documented due to the abundance of historical documents for this period. During the Neolithic Age, local cultural communities developed in the central southern region of the Huai River Valley (Anhui), while other communities in the valley were related to the four surrounding cultural regions,[14] including the Haidai Region in the northeast, the Jiangzhe Region in the southeast, the Central Plains Region in the northwest, and the Jianghan Region in the southwest (Figure 1). The cultural sequences in these regions are shown in Table S1. During the Bronze Age, the valley was under the control of the Xia, Shang, and Zhou Dynasties, with onset times of around 2070, 1600, and 1046 BC, respectively.[65–67]

Archaeological and pollen datasets

Archaeological sites of settlements

Data on a total of 4484 archaeological sites in the Huai River Valley were collected from published Chinese Cultural Relics atlases for 5 provinces (Henan, Shandong, Jiangsu, Anhui and Hubei).[36–40] These atlases document the archaeological findings of the second national cultural survey undertaken by the Chinese government during the 1980s, and they include much information about archaeological sites (e.g., name, location, area, culture type, cultural depth, and archaeological remains).

Around 97% of the archaeological sites belong to cultural types covering an interval of less than 2,000 years (Figure 1D; Table S3), and they were assumed to persist throughout their cultural periods (Table S1). The other 3% sites with unclear Neolithic cultural types were assigned to respective 1,000-year time windows according to the proportions of the sites with clear cultural types in different millennia,[36–40] as the overwhelming percentages of sites with clear cultural types essentially determine the temporal changes of the sites.

Around 80% of the sites have documented residential area values, while the median values of these known sites were adopted for the unknown sites under the same cultural types.[36–40] To reduce uncertainties caused by using the same value to represent site areas in different cultural periods, only known sites covering a single cultural type were used as references.

The spatial distributions of archaeological sites in the Huai River Valley evolved from scattered to widespread (Figure S1). During 8–7 ka BP, archaeological sites were mainly distributed in several areas of the western, southern, and northeastern valleys, which correspond to four different cultural groups (NW, AH, SE, NE) developed in the Huai River Valley (Figure 1B). At 7–6 ka BP, the expansion of archaeological sites

occurred mainly in the western valley with the rise of the Yangshao Culture in the NW group. During 6–5 ka BP, the greatest increases in the density of archaeological sites in the northeastern and central southern valley were due to the significant spread of the Dawenkou Culture from the NE group to the western and southern parts of the valley, and the diffusion of the Middle Neolithic Culture from the AH group to a larger area in the southern valley. At 5–4 ka BP the large-scale expansion of archaeological sites across the valley (the southeastern part), can be explained by the spread of the Longshan Culture from the NW group to the southeastern valley, and the Late Neolithic Culture from the AH group to the northern valley, in opposite directions. After 4 ka BP, the distribution pattern of archaeological sites essentially remained the same as before, when different local cultural groups integrated across the valley and fell under the rule of the same dynasties (i.e., Xia, Shang and Zhou) from the NW group.[36–40]

Archaeological sites with crop seeds

Data on a total of 467 archaeological sites with crop seeds around and within the Huai River Valley were compiled from the published literature.[12,24,67–69] They were used as inputs to the land use type sub-model (Figure 1C; Table S2). The available literature comprehensively documents the location, culture, and type of crop plant remains of the archaeological sites. 46% (n=217) of these archaeological sites recorded crop plant types and the corresponding seed quantities based on the floatation of carbonized crop seeds,[12,24] which can be directly used to calculate the proportion of rice cultivation at an archaeological site. The flotation results of the other 250 sites only distinguished the crop plant types, and the results showed that there was only one type, either dry or rice, at the archaeological site; therefore, it can be inferred that the rice cultivation ratio at the site was either 100% or 0%. The archaeological sites were assigned to respective 1,000-year time windows according to the duration of their cultural types in different millennia (Table S1).

From 8 to 2 ka BP, the average rice percentage at archaeological sites remained at ~40%, except for a pronounced decrease (27%) at 4–3 ka BP (Figure S7). The spatial distribution of the rice percentage at archaeological sites with crop-plant remains essentially followed a pattern of high values in the southeast and low values in the northwest (Figure S7).

Cultural parameters

The socioeconomic parameters for land use need, type, and allocation sub-models in PLUM were collected from the published archaeological literature, and the values used for the Huai River Valley are listed in Table S4.

The value ranges of residential area per person were set according to the research on typical archaeological sites in northern China.[43]

The average food need per person was estimated from an individual's minimum annual nutritional requirements based on calories,[70] because agricultural food was assumed as the only source of human diet in PLUM. The estimated value of 300 kg/year was regarded as a constant for the study period here, as no significant changes in human physiognomy or physiology occurred during the Holocene.[71]

The value ranges of yields per unit area for dry and rice cultivation were obtained from a combination of archaeological research (e.g., phytolith remains),[72,73] historical documents,[74] and observations of modern slash-and-burn agriculture.[75,76] The average crop yields per unit area for different 1000-year intervals were further calculated and applied in the cropland reconstruction.

The fallow intervals for the periods of >7 ka BP and 7–5 ka BP were set according to different fallow types (long duration forest fallow, bush fallow, and short fallow) determined by *Wang*,[42] based on studies of typical archaeological sites; while the value for 3–2 ka was estimated from records of the Han Dynasty and modern slash-and-burn agriculture.[77,78] The corresponding value for 4–3 ka BP was obtained by linear interpolation of the above results.

The threshold value (10 km) of the available area for cropland was based on an estimated maximum time (2 h) that a human can reasonably be expected to spend on travelling to the agricultural fields in one day.[79]

Environmental variables

Spatial data throughout the Huai River Valley for the residential area sub-model were derived from digital maps of modern elevation, soil type, and river system. Elevation data, represented by a grid layer with a horizontal resolution of 90 m and a vertical resolution of 1 m, were obtained from the Shuttle Radar Topography Mission (SRTM) website (http://srtm.csi.cgiar.org/). The vector layers of soil type and river system, with scales of 1:1,000,000 and 1:4,000,000, were obtained from the National Earth System Science Data Center (http://www.geodata.cn/). The grid layers of slope and aspect were directly derived from the elevation data using Geographic Information System (GIS) software (ArcGIS 10.2), while the grid layers of vertical and horizontal distances to river system were further calculated based on the river system and elevation data. All these vector and grid layers comprising the environmental variables were converted or re-sampled to gridded data with a constant resolution of 0.01°×0.01° using the uniform WGS_1984 projection.

Pollen records

Fossil pollen data were obtained from *Herzschuh* et al.[80] and *Li* et al.[81] within the certain distance range (about 700 km) from the Huai River Valley (Figure S8; Table S5). A total of 20 sites were selected using the following criteria to ensure data quality and an adequate site-distribution: (1) The record had more than three chronological controls with at least two independent dates (e.g., radiocarbon). (2) Following the methods of Webb59,[82] only samples with a date within 1 kyr or bracketed by dates within 6 kyr were retained. (3) The duration of the record exceeded 5 kyr, and the record included samples younger than 1 ka BP, as required to calculate the anomalies. (4) The sampling resolution was less than 400 years (5) Samples with pollen counts <200 were excluded.

All radiocarbon dates were recalibrated using the IntCal20 calibration curve and interpolated to sample levels using the R package 'clam'.[83,84] In addition to ages derived from direct dating, other chronological controls, such as annual lamination counts, biostratigraphic controls, and core-top ages from pollen databases,[85] were also included in the interpolation.

The modern pollen dataset used for transfer function development comprised 1,863 surface samples, compiled from *Li* et al.[81] and the East Asian Pollen Database.[86] The distribution of surface samples covers the whole China and it represents climate conditions from cold temperate to tropical (Table S5).[86] This wide ecological and climatic range spans the range of Holocene climate change in the Huai River Valley. Modern climate variables, including the mean annual temperature (MAT) and mean annual precipitation (MAP), were determined by thin-plate spline interpolation with latitude, longitude, and elevation covariates using a 0.5° gridded monthly mean climate dataset (1950–2010, CRUTS v4.01).[87]

PLUM model and improvements

The Past Land Use Model (PLUM) is a useful tool for quantitatively reconstructing the areas and distributions of past land use in a single cropping system, according to the intensity and spatial distribution information of human activity provided by archaeological sites (detailed model descriptions can be found in *Yu* et al.[30,31]; *Yu* et al.[32]).

More than one cropland type exists in a mixed cropping system and their different yields affect the size and distribution of cropland intensity. A sub-model named 'land use type' was added to the new version of PLUM (Figure S2), based on crop seed floatation data from archaeological sites which well represented the composition of local cultivation types.[12] The proportions of dry and rice cultivation in archaeological sites (expressed by rice cultivation percentages) were first calculated according to the numbers of two types of carbonized crop seeds remains. Then, the spatial distribution of rice cultivation percentage across the study region was interpolated using the inverse distance method (IDW) according to the proportions of rice cultivation from the archaeological sites, and the potential yields of different cropland types in the study region were further obtained in the land use type sub-modell.

Second, the actual crop yield needs for all archaeological sites were calculated in the land use need sub-model. This sub-model was previously used for estimating the total cropland and living areas in the study region, based on the assumption that the food requirements of the population are entirely supplied by cultivated plant sources, since it is still difficult to quantitatively estimate the contributions of animal and wild plant resources to the Holocene human food sources based on current archaeological records. In the new version of PLUM, the actual total crop yield need (Y_a) for the settlements of the study region was calculated using the Equation 1, which was composed by dry or/and rice cultivation yields.

$$Y_a = \left[\left(A_r / A_p\right) \times F_p\right] \times \left[\left(T_f + T_c\right) / T_c\right] \quad \text{(Equation 1)}$$

Here, A_r is the total residential area, including the houses, barns, gardens, and common spaces used for human social activity in the archaeological site; A_p is the average residential area per person. The former is usually inferred by archaeologists according to the total excavation area of each site, while the latter is always obtained by tomb and settlement analysis of the excavated sites, and they are together used to estimate the total population size in the site. F_p is the food required per person; and T_f and T_c are the fallow and tillage periods, respectively, in a single cultivation cycle, as the fallow system was widely adopted in prehistoric slash and burn agriculture to maintain field productivity.[42]

Third, the potential distributions of human occupation (expressed by rank values) were predicted in the residential area distribution sub-model, and the previous version of this sub-model was directly adopted in the new version of PLUM. The prediction was according to the relationship between different environmental variables and the distribution of recorded archaeological sites, and the weighted overlay method was adopted by three steps. (1) The class weights indicate the sequence of the relative importance of different environmental variables for the distribution of human activity in the study region, and they are set according to the difference between the cumulative frequency distributions of each environmental variable in two groups (locations of all grids vs. archaeological sites). (2) The spot weights indicate the degree of dependency of human activity on various ranges of a specific environmental variable in the study region, and they are set based on the frequency distributions of archaeological sites in different sub-ranges of each specific environmental variable. (3) Two types of weight of a specific environmental variable layer are multiplied to produce the total weight values for the grids across the study region, and all the total weighted layers are summed to one layer with a standardized rank of 0–100%, which represents the potential distribution of human activity from low to high in the study region.

Finally, the actual cropland areas estimation under different cultivation types and their spatial distributions were realized by the improved land use allocation sub-model. (1) The total actual crop yield need of a particular archaeological site from the land use need sub-model is distributed to the appropriate grids around the archaeological site within a specific radius. The distribution follows the principle that the grids with higher rank values predicted by the residential area distribution sub-model are first selected as suitable cultivation areas, and the allocation is also constrained by the potential maximum crop yield in each grid across the study region, as estimated by the land-use type sub-model. (2) The actual cropland areas of different cultivation types in each grid are calculated based on crop yield per unit and the ratios of different cultivation types predicted by the land-use type sub-model.

Overall, the first three sub-models (land use need, land use type and residential area sub-models) provide inputs (such as total crop yield need, potential distributions of crop yields under different cultivation types and human occupation) for the land use allocation sub-model, and the last land use allocation sub-model outputs the sizes and distributions of regional croplands under different cultivation types.

Paleoclimate reconstruction

The Modern Analog Technique was adopted for the quantitative reconstruction of annual mean temperature and precipitation from 8 to 2 ka BP,[88] based on fossil pollen data, and implemented in the R package 'Rioja'.[62] First, according to the squared chord distance (SCD),[89] fossil pollen samples were directly matched with modern datasets using the dissimilarity of biome score compositions. Then, the dissimilarity-weighted mean climate of the seven closest modern analogues was assigned to the fossil sample.[90]

During the reconstruction, PFT (plant functional type) scores rather than pollen taxa were used in the dissimilarity calculation,[91,92] because PFTs (i.e., groups of dominant plants characterized by common phenological and climate constraints) can be used to reduce poor analogue cases and non-climatic influences,[93] and hence provide a more accurate and consistent reflection of the climate.[91,92] PFT scores were calculated using the taxa–PFT matrices in the biomization procedure for East Asia.[94] In this study, only fossil samples with close analogues under certain dissimilarity thresholds were retained. The thresholds were determined based on the trade-off between the precision/accuracy of the reconstruction and the utility for the majority of samples.[95] A relatively low SCD (<0.5 throughout the Holocene) between fossil samples and modern analogues indicates a good analogue situation,[96] ensuring the reliability of the reconstructions.

The Modern Analog Technique performed well in the MAT and MAP reconstructions, as a high coefficient of determination (R^2>0.8) was produced based on leave-one-out cross-validation using the modern pollen datasets (Figure S9), while the comparable spatial patterns between observed and reconstructed modern MAT and MAP further support the application of the Modern Analog Technique to the reconstruction of Holocene climatic factors (Figure S10).

Following *Marsicek* et al.,[97] all the significant reconstructions were converted to anomalies using the mean of the latest 1000 years, linearly interpolated to 200-year bins, generated into regional composites of MAT and MAP, and finally averaged into different 1000-year intervals. The anomalies were further overlaid onto grid layers of modern temperature and precipitation to obtain corresponding grid layers of past millennia.

The errors during the reconstruction procedure were fully considered, including three main sources: (1) Errors in modern biome-climate calibration and the application for each sample (sample-specific errors); (2) temporal interpolation errors for each pollen site; and (3) spatio-temporal stack uncertainties. For each source, the Monte Carlo or bootstrap resampling approach was used to assess the uncertainty. 95% confidence limits for the reconstructed climate curve were produced by combining all the errors.

The reconstructed MAT and MAP during 8–2 ka BP of the Huai River Valley were warmer (+0.16°C) and wetter (+187 mm) than today. The temporal changes in both MAT and MAP can be divided into two stages: a relatively higher level before 4 ka BP (+0.26°C and +199 mm than today), and a decrease after 4 ka BP (-0.02°C and +168 mm than present). The trend of decreasing precipitation after 4 ka BP was more significant than that of temperature (Figure 5B).

Previous studies reveal that a "South-North dipole pattern" of precipitation existed in China during the Holocene.[98–100] As the Huai River Valley is located in the central China, it would potentially distribute across the dipole junction zone with complex climate condition. Here, the pollen records used for MAP reconstruction of the Huai River Valley were divided into two groups according to their locations (north and south of the valley) (Figure S8A), and the synchronous changes of MAP occurred between the north and south groups during the Holocene indicating most of the valley distributed in the north part of "South-North dipole pattern" (Figure S8B). The reconstructed MAP change in the Huai River valley basically followed the trend of northern China, and such pattern is further validated by the simulation results of TraCE-21k.[98,99] Overall, the reconstructed climatic factors in the Huai River Valley could be taken as reliable references for further regression analysis.

Reconstructing cultural intensity

Kernel density estimation (KDE) is a nonparametric approach for estimating probability density functions, which is frequently employed to portray the spatial distribution density of geographical occurrences.[101] KDE can smooth the influence of individual events within the dataset, yielding density estimates for each location, and it enables the identification of spatial clustering trends among events, thus has been widely applied in archaeological studies to show past human activity distribution.[102,103] Here, the kernel densities of archaeological sites from four cultural groups in the Huai River Valley were used to quantitatively express the pattern and intensity of different cultures. Processing was conducted in ArcGIS by converting point features to grid layers (0.1°×0.1°) across the Huai River Valley (Figure S5).

Among the four cultural groups in the Huai River Valley, the intensities of the NW, NE, and AH groups all increased before 4 ka BP, except SE group (Figure 5). After 4 ka BP, four regional cultural groups were integrated into a single group,[36–40] whose intensity increased continuously.

Multiple regression analysis of climatic and cultural factors

Multiple regression analysis is widely to solve the problem of multiple independent variables affecting a dependent variable, and the coefficients of different independent variables reflect the strength of their impacts on the dependent variable.[104] Temperature and precipitation are key natural climatic factors that determine the potential regional crop yield,[105] while cultural intensities are the main social factor that influences the actual crop yield.[106] Moreover, changes in both climatic factors and cultural intensities have spatiotemporal characteristics. Here, the grid layers (0.1°×0.1°) of cropland type and cropland area across the valley were taken as the dependent variables, respectively, while the grid layers of MAT, MAP and cultural intensity were used as independent variables, therefore, the relative roles of external climatic and internal social factors played in distributions of cropland type and area during the prehistoric period were revealed.

QUANTIFICATION AND STATISTICAL ANALYSIS

The average residential areas in archaeological sites (from 154 to 2,899) during each millennium from 8 to 2 ka BP, as shown in Figure 2, were represented as mean ± SEM. The average population in archaeological sites, total population, and total cropland area of the Huai River Valley were calculated based on the residential areas and three different values of residential area per person in archaeological sites during each millennium (Table S4), therefore, three values (mean, minimum and maximum) were obtained for these variables and shown in Figure 2.

As the reconstructed northern boundary of rice-dominated cropland during each millennium in the Huai River Valley spanned different latitudes (Figure 3), its temporal change was shown by the mean, minimum and maximum values of its latitude in Figure 5.

The multi-regression analysis clarifying the controlling factors of cropland type and area distributions was performed using PASW Statistics software, and the grid layers (0.1° × 0.1°) of all dependent (cropland type and cropland area) and independent (MAT, MAP and cultural intensity) variables were standardized to the range of [0, 1] during the analysis. The regression analyses were carried out by four different cultural groups in the Huai River Valley (NW, NE, AH and SE) (Figure 1) separately during the Neolithic period, therefore, the regression coefficients of four different cultural groups during each millennium were further calculated as the mean and the corresponding values located at 10%, 25%, 75%, and 90% positions in Figure 4.